Diffraction imaging: The limits of partial coherence

Bo Chen,[1] Brian Abbey,[1,2,*] Ruben Dilanian,[1] Eugeniu Balaur,[2] Grant van Riessen,[2] Mark Junker,[2] Chanh Q. Tran,[2] Michael W. M. Jones,[2] Andrew G. Peele,[2] Ian McNulty,[3] David J. Vine,[4] Corey T. Putkunz,[1] Harry M. Quiney,[1] and Keith A. Nugent[1]

[1]*ARC Centre of Excellence for Coherent X-ray Science (CXS), School of Physics, The University of Melbourne, Victoria 3010 Australia*

[2]*ARC Centre of Excellence for Coherent X-ray Science (CXS), Department of Physics, La Trobe University, Victoria 3086 Australia*

[3]*Center for Nanoscale Materials, Argonne National Laboratory, Argonne, Illinois 60439, USA*

[4]*Advanced Photon Source, Argonne National Laboratory, Argonne, Illinois 60439, USA*

(Received 2 August 2012; published 3 December 2012)

Coherent diffraction imaging (CDI) typically requires that the source should be highly coherent both laterally and longitudinally. In this paper, we demonstrate that lateral and longitudinal partial coherence can be successfully included in a CDI reconstruction algorithm simultaneously using experimental x-ray data. We study the interplay between lateral partial coherence and longitudinal partial coherence and their relative influence on CDI. We compare our results against the coherence criteria published by Spence *et al.* [Spence *et al.*, Ultramicroscopy **101**, 149 (2004)] and show that for iterative *ab initio* phase-recovery algorithms based on those typically used in CDI and in cases where the coherence properties are known, we are able to relax the minimal coherence requirements by a factor of 2 both laterally and longitudinally, potentially yielding significant reduction in exposure time.

DOI: 10.1103/PhysRevB.86.235401 PACS number(s): 61.05.C−, 87.59.E−

I. INTRODUCTION

High-resolution x-ray imaging continues to be the subject of considerable research. One relatively recent development is coherent diffraction imaging (CDI)[1] in which a far-field coherent diffraction pattern is inverted to produce a high-resolution image that contains both amplitude and phase information. It is anticipated that x-ray CDI will continue to become an important imaging method for imaging samples with a resolution in the range of one to ten nanometres.[2,3] CDI has been applied in material science[4–6] and biology[7–12] successfully.

A particular motivation for the development of CDI lies in its potential to provide high-resolution images using sources such as x-ray free electron lasers (XFELs),[13] where it is anticipated that it may ultimately be possible to image single molecules. Recent work has shown that it is possible to determine biomolecular structures with XFELs.[14]

While third-generation synchrotron sources can be used effectively for CDI, the incident light requires significant spectral and spatial filtering in order to achieve the necessary lateral and longitudinal coherence,[15] in a large fraction of the x-rays in the beam being discarded. Even XFELs are partially coherent and have a coherence length significantly less than that of visible lasers.[16] A reduction in filtering requirements would therefore decrease the required exposure time. Recent work has shown that it is possible to use either sufficiently well characterized partially coherent light[17] or incident light with a significant, but known, bandwidth;[18,19] both methods promise imaging with a significantly shorter exposure time. While the above cited papers show that a certain level of partial coherence may be tolerated, there must clearly be limits to the extent that partial coherence can be compensated for in a CDI experiment. In the present paper, we first review the theory underpinning the partially coherent approaches as a precursor to our report of a systematic experimental study of the limits to which lateral and longitudinal coherence may be tolerated in CDI.

II. THEORY

Analysis of CDI typically assumes that the incident light is fully coherent. An analysis of CDI in the case of partially spatially coherent incident light has been performed.[15] This work used the formulation of optical coherence theory to describe and analyze the diffraction process. Here we review the essential points in that analysis.

The diffracted intensity $I(\mathbf{r}')$ in the far field of an object described by an amplitude transmission function $T(\mathbf{r})$, where $\mathbf{r}$ is the position vector in the sample plane, illuminated with light described by a mutual optical intensity (MOI), $J(\mathbf{r_1},\mathbf{r_2})$ is given by

$$I(\mathbf{r}') \propto \int J(\mathbf{r}_1,\mathbf{r}_2)T(\mathbf{r}_1)T^*(\mathbf{r}_2) \times \exp\left[-2\pi i \frac{\mathbf{r}'\cdot(\mathbf{r}_1-\mathbf{r}_2)}{\lambda z}\right] d\mathbf{r}_1 d\mathbf{r}_2, \quad (1)$$

where $\mathbf{r}'$ is the position vector in the detector plane, λ is the wavelength of the incident light, and z is the distance between sample and detector, and we have suppressed the irrelevant prefactors on the right-hand side of Eq. (1). In the limit of complete incoherence ($J(\mathbf{r_1},\mathbf{r_2}) \rightarrow I_0\delta(\mathbf{r_1}-\mathbf{r_2})$, where I_0 is the intensity of the light field), it is clear that all structural information about the scattering object is lost. It follows that there must exist a point at which the light is sufficiently partially coherent that the properties of the scattering function cannot be recovered.

Equation (1) describes the data that will be obtained but offers little insight into how the object may be recovered. Whitehead *et al.*[17] have shown that it is possible to use the coherent mode formulation of partial coherence[20] to develop a suitable iterative process.

The coherent mode formulation of coherence theory was proposed by Wolf[20] and it describes the MOI of an

electromagnetic field in the form

$$J(\mathbf{r}_1,\mathbf{r}_2) = \sum_{n=1}^{N} \eta_n \phi_n(\mathbf{r}_1)\phi_n^*(\mathbf{r}_2). \quad (2)$$

Here, η_n are a real, non-negative numbers representing occupancy of the mode $\phi_n(\mathbf{r})$, where there are N such modes in the field. The modes are themselves mutually incoherent. Using this formulation, the intensity of a partially coherent field can be reduced to

$$I(\mathbf{r}) = \sum_{n=1}^{N} \eta_n I_n(\mathbf{r}), \quad (3)$$

where $I_n(\mathbf{r})$ is the intensity produced by the n$^{\text{th}}$ mode. It is possible to measure the coherence of the x-ray beam in some detail[21] and decompose it into its coherent modes.[22] Armed with this information, it is possible to perform a reconstruction of the sample using the methods described in Ref. 17. A comparable method may be applied to longitudinal coherence in which the illumination is divided into a series of mutually incoherent modes, with each mode of different wavelength.[19] In the present paper, we report an experimental investigation into the limits of these approaches and also the extent to which it is possible to recover images from diffraction by fields that are both partially laterally and longitudinally coherent.

III. COHERENCE REQUIREMENTS

A number of analyses have been published on the coherence requirements for successful CDI. Spence *et al.*[23] have suggested using a theoretical argument that the lateral coherence length should be at least twice the greatest spatial extent of the object. Williams *et al.* have used simulations[15] and experiments[24] to find that if the reconstruction algorithm implicitly assumes full coherence, then the ability to reconstruct the data is limited even for very small deviations from perfect coherence. The criteria proposed in Ref. 23 may therefore be optimistic for an algorithm that assumes complete coherence.

In this work, we will characterize our coherence properties in terms of the criteria of Spence *et al.*.[23] We therefore introduce the dimensionless parameter, S_s, which is the ratio of the lateral coherence length (a precise definition of which is supplied in the next section) to twice the maximum linear extent of the object, L:

$$S_s = \frac{\sigma_{s,x}}{2L}. \quad (4)$$

The longitudinal coherence length is determined by the bandwidth. Here we use the definition for the longitudinal coherence length as

$$\sigma_l = \frac{\lambda^2}{\Delta\lambda} = \frac{\nu}{\Delta\nu}\lambda, \quad (5)$$

where $\Delta\nu$ in Eq. (5) is the full width at half maximum of the spectrum. For an object of maximum dimension L, the requirement that light from both edges of the scattering object experience a path difference of less than one longitudinal coherence length when scattered at an angle θ is $\sigma_l > L\sin\theta$. The angle of scattering determines the resolution δ of the reconstruction via $\delta = \lambda/2\sin\theta$ and so[3] combining these expressions, the requirement on longitudinal coherence length for CDI is resolution dependent via $\sigma_l > \frac{L}{2\delta}\lambda$. This is essentially the longitudinal coherence requirement identified in Ref. 23 and accordingly, we will characterize the longitudinal coherence for our data via the dimensionless parameter

$$S_l = 2\sigma_l\frac{\delta}{\lambda L}. \quad (6)$$

IV. ANALYSIS OF THE INCIDENT FIELD

To characterize the source, we need to measure the MOI function of the source and the spectrum. The MOI function is a four-dimensional function, which is hard to measure completely. Earlier experimental work[21] has shown that for the x-ray source used in this work, the MOI function is very closely approximated by the Gaussian-Schell model that has been extensively studied theoretically elsewhere.[25] The Gaussian-Schell model is described by the form

$$J(\mathbf{r_1},\mathbf{r_2}) = I_m \exp\left(-\frac{x_1^2+x_2^2}{4\sigma_{I,x}^2}\right)\exp\left(-\frac{y_1^2+y_2^2}{4\sigma_{I,y}^2}\right) \times \exp\left[-\frac{(x_1-x_2)^2}{2\sigma_{s,x}^2}\right]\exp\left[-\frac{(y_1-y_2)^2}{2\sigma_{s,y}^2}\right], \quad (7)$$

where I_m is the maximum intensity, x and y are horizontal and vertical directions, respectively, in the sample plane perpendicular to the propagation of light, $\mathbf{r} = (x,y)$ is a vector in that plane, and $\sigma_{I,x}$ and $\sigma_{I,y}$ characterize the width of the intensity distribution in the x and y directions, respectively. $\sigma_{s,x}$ and $\sigma_{s,y}$ are the lateral coherence lengths of the light in x and y directions, respectively. The variation of the intensity of the light at the sample plane is sufficiently slow that it can be regarded as essentially uniform over the sample and so we can set $\sigma_{I,x},\sigma_{I,y} \to \infty$. The vertical coherence for the synchrotron is known to be very high, and so we also take $\sigma_{S,y} \to \infty$. The remaining unknown is $\sigma_{s,x}$, and so it is to be measured in the experiment. The analytical form of the coherent modes of the Gaussian-Schell model have been calculated and tabulated[25] and these can be used in the reconstruction using the measured value of $\sigma_{s,x}$.

The overall experimental coherence parameters may be obtained from a Youngs double slit experiment. The fringe separation determines the slit separation, the fringe envelope determined the slit width, the central fringe visibility determines the spatial coherence and the variation of the fringe visibility determines the longitudinal coherence. The relative independence of these measurable parameters allows their reliable extraction using a variety of methods.[26,27]

Our CDI algorithm for partially coherent light is based on previously published work.[17,19] We first use 50 steps of hybrid-input-output (HIO) and 150 steps of error reduction (ER) to obtain a low-resolution reconstruction,[28] and then use charge flipping[29] and shrink wrap[30] to run the reconstruction for several hundreds of steps to get the final result.

V. EXPERIMENT AND RESULTS

The experimental setup is illustrated in Fig. 1. The experiment was carried out at beamline 2-ID-B of the Advanced

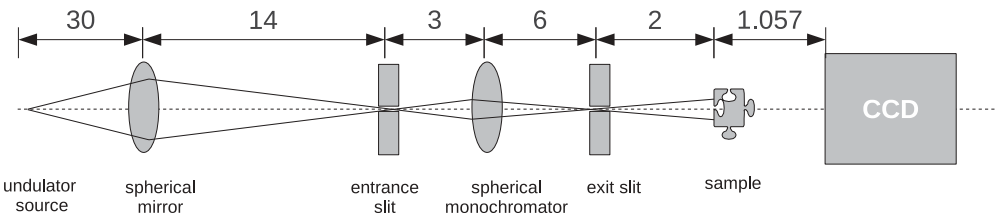

FIG. 1. Schematic of the experimental setup at 2IDB beamline of APS. The widths of the entrance and exit slits can be changed to change the coherence of the source. The monochromator can be removed to get a "pink" beam.

Photon Source (APS)[31,32] using a conventional CDI setup. An x-ray beam with energy of 1.4 keV was used. The longitudinal coherence was controlled by the spherical grating monochromator and the width of the entrance slit, while the lateral coherence length was controlled by the width of the exit slit.

The double slit and sample were manufactured using a focused ion beam. In our experiment, the nominal separation of the double slit was 12 μm, with the width of each slit $w = 1$ μm. The sample was made of 6-μm thick gold film. The maximum dimension of the sample (distance across the diagonal) was 12 μm. Electron micrographs of the front and back of the sample are given in Figs. 2(a) and 2(b), respectively. The sample and the slit pair were installed in the same sample stage after a beam defining aperture (BDA) in the vacuum chamber. A CCD with 2048 $\times$ 2048 pixels, each pixel 13.5 $\times$ 13.5 μm^2, was placed 1057 $\pm$ 1 mm downstream from the sample plane.

The double slit was first illuminated by the most coherent light possible from our experimental arrangement by minimizing the widths of the entrance and exit slits (20 and 5 μm, respectively). The procedure of fitting the interference pattern in reference[33] was used yielding a slit separation of $d = 11.57$ μm and a slit width of $w = 1.02$ μm. Because the thickness of the sample (6 μm) is much larger than the width of the slit, it is hard to control the fabrication very precisely and there is discrepancy between the measured size and the nominal one. The measured values were used for the remainder of the analysis.

The coherence properties of the source were then measured for a range of entrance and exit slit widths. To obtain the broadest possible bandwidth ("pink beam"), we moved the spherical grating out of the beam and opened the entrance slit to its largest width (around 450 μm). For each experimental setup, we first obtained and fitted the Young's interference pattern to measure the coherence lengths. Figure 3 plots these information.

Note that at the smallest slit dimensions, an entrance slit width of 20 μm and the exit slit width of 5 μm, the lateral coherence length is larger than the size of the sample, and the bandwidth is less than 1.5×10^{-3} ($\sigma_l > 590$ nm). The lateral coherence corresponds to a value of $S_s = 0.8$. We reconstruct

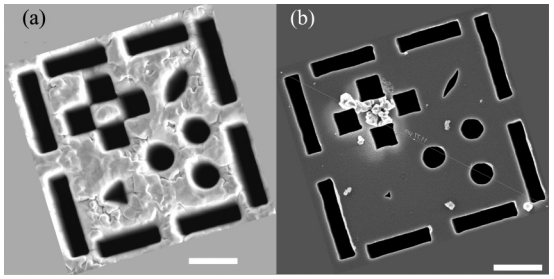

FIG. 2. (a) The scanning electronic microscopy (SEM) image of the sample. (b) The backside of the sample. The scale bar is 2 μm. The triangular feature is largely absent on the backside of the sample and so this feature has not been fully etched through the substrate.

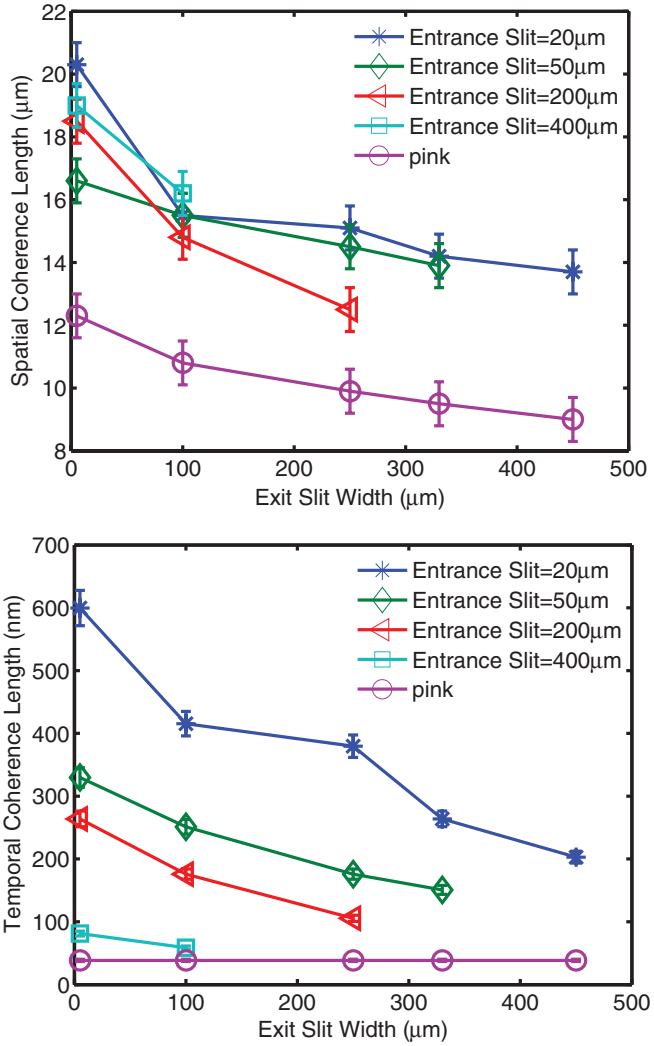

FIG. 3. (Color online) Fitted lateral coherence length $\sigma_{s,x}$ (top) and longitudinal coherence length σ_l (bottom) for different entrance/exit slit combinations from double slit interference pattern. The data for some exit slit widths are missing due to the saturation of the CCD when even the fastest shutter speed is used.

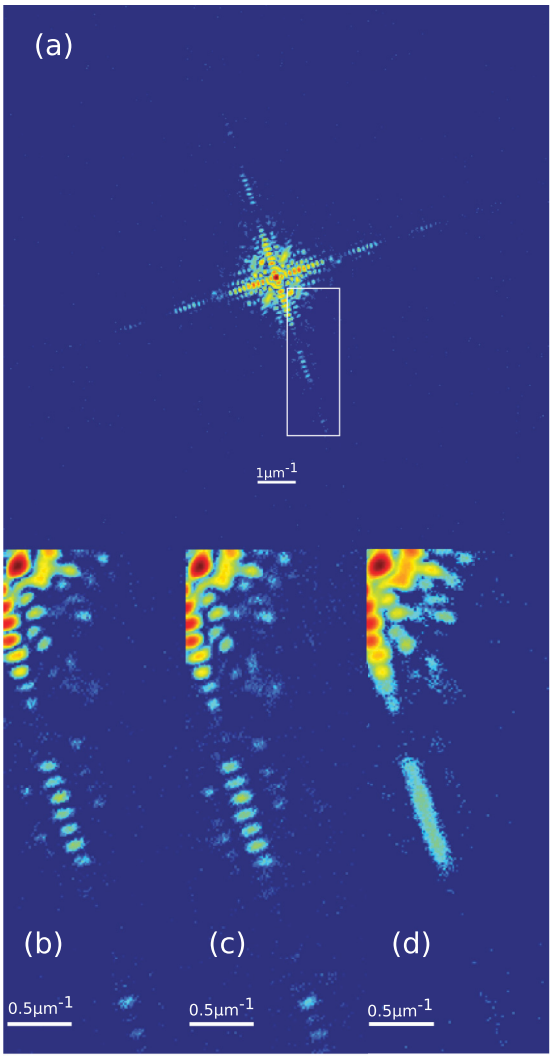

FIG. 4. (Color online) (a) The diffraction pattern of the fully coherent mode (b)–(d) are the diffractions in the same area bounded by the white box in (a) for slit settings as $S_l = 5.78$ and $S_s = 0.87$, $S_l = 0.73$ and $S_s = 0.55$ and $S_l = 0.37$ and $S_s = 0.39$, respectively. The decrease in the contrast of the diffraction is readily seen. All data are shown in logarithmic scale.

images to a resolution of 100 nm and so $S_l > 8.3$. That is, the lateral coherence length is 0.8 of the value suggested by Spence *et al.*, but the longitudinal coherence length is at least 8.3 times the minimum requirement. While the lateral coherence falls short of the value that might be termed completely coherent, this illumination will be used as the benchmark; it is the highest coherence that the beamline can deliver at this energy.

As the widths of the entrance and exit slits in the experimental system increase, the illumination becomes less laterally and longitudinally coherent, the illumination becomes increasingly laterally and/or longitudinally partially coherent; it is to be anticipated that a CDI reconstruction under a fully coherent assumption will ultimately fail. Sample diffraction patterns are shown in Fig. 4. To compare the data with different illumination, the same part in the area of the white box in Fig. 4(a) for three combinations of slit width setups are shown in Figs. 4(b)–4(d).

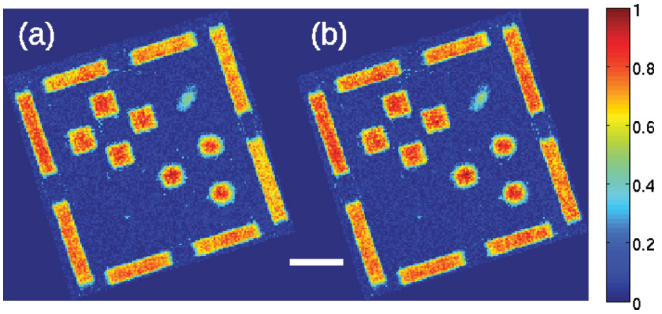

FIG. 5. (Color online) The reconstruction of the amplitude of transmission function of the sample. The entrance slit width was set at 20 μm and exit slit was set at 5 μm. (a) CDI reconstruction assuming perfect coherence. (b) Partially coherent CDI reconstruction. No obvious difference can be observed in the two reconstructions, meaning that the effect of partial coherence is negligible in this experimental setup. The scale bar is 2 μm. The color scale is linear between an amplitude transmission of 0 (perfect absorption) and 1 (complete transmission).

The reconstructed result is shown in Fig. 5 for the most coherent data. Figure 5(a) shows the result of the CDI reconstruction assuming fully coherent and Fig. 5(b) shows the result of the appropriate partially coherent algorithm. In this case, a good reconstruction is obtained and there is no obvious difference between the reconstructions assuming full coherence and one that properly accounts for the partial coherence; the effect of the partial coherence is, for this high-contrast sample at least, negligible. From the reconstruction, we can see that triangle shape in the sample is not well reconstructed, consistent with this shape not penetrating completely through the substrate, as can be seen via a comparison between Figs. 1(a) and 1(b).

Data were obtained for the full range of experimental conditions and the partially-coherent CDI algorithm was used to reconstruct the sample from the diffraction patterns. The highest coherence data set was used as a benchmark and all other reconstructions were compared to it using the metric R defined as

$$R = \frac{\sqrt{\sum_{i,j} \left\| T^P_{i,j} - T^C_{i,j} \right\|^2}}{\sum_{i,j} \left\| T^C_{i,j} \right\|}, \tag{8}$$

where the reconstructed complex data set, $T^P_{i,j}$ was compared with the high coherence one $T^C_{i,j}$.

A representative sample of the reconstructed images is shown in Fig. 6. A summary of the results is shown in Fig. 7 in which all of the data is plotted against the values of S_s and S_l. The value of R is shown as the color of the corresponding point on the plot.

VI. DISCUSSION

The threshold for an acceptable image is somewhat subjective. Here we choose that a requirement of $R < 0.04$ as a reasonable criterion for an acceptable image. For example, the reconstruction shown in Fig. 6(e) is at the threshold for acceptance ($R = 0.036$) whereas the image in Fig. 6(f) is, by this criterion, not acceptable($R = 0.06$).

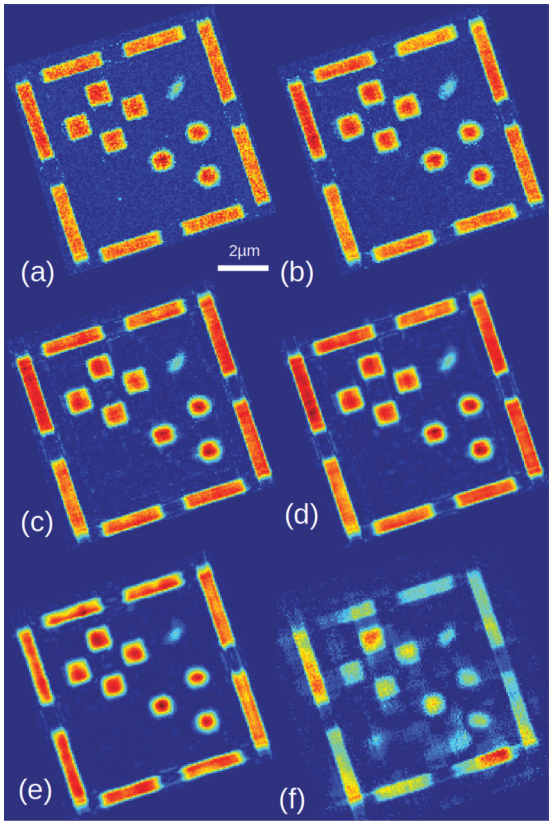

FIG. 6. (Color online) Reconstructed amplitude of the transmission function using different entrance/exit slit combinations. (a) $S_l = 5.78, S_s = 0.87$; (b) $S_l = 3.91, S_s = 0.65$; (c) $S_l = 0.73, S_s = 0.55$, (d) $S_l = 0.57, S_s = 0.69$; (e) $S_l = 0.37, S_s = 0.39$; (f) $S_l = 0.37, S_s = 0.33$. The reconstructed results is acceptable until (d). In (e), the quality of the reconstruction degrades as the $S_s < 0.5$. While in (f), the reconstruction fails. The scale bar is 2 μm and the color scale is same as for Fig. 5.

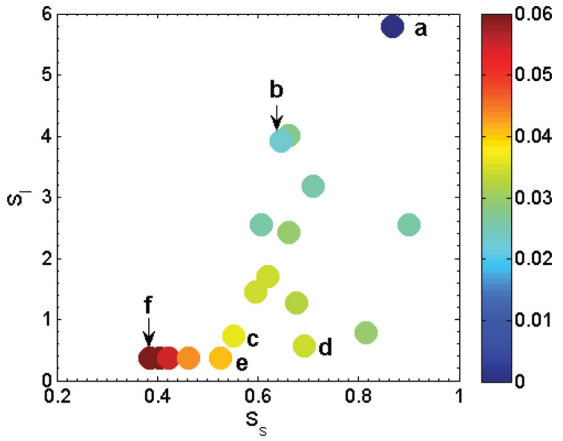

FIG. 7. (Color online) R values of different setups. The R values in Figs. 6(a)–6(f) are labeled accordingly here. We choose $R < 0.04$ as a criteria of a "good" reconstruction. By this criterion, (a)–(e) are acceptable, (f) is not acceptable, which is consistent with Fig. 6.

Using this analysis, an examination of Fig. 7 indicates that by the criterion above, acceptable reconstructions were obtained for all available coherence conditions provided $S_s > 0.5$. Our experimental arrangement did not deliver light with high lateral coherence and low longitudinal coherence and so this gap was explored using simulations, as shown in Fig. 8. In these simulations, the conditions were identical to those in the experiment. The simulated lateral coherence length was 20 μm ($S_s = 0.83$) and the longitudinal coherence lengths were assumed such that $S_l = 1.67, 0.72$, and 0.33. It can be seen that the reconstructions are reasonable for the first two conditions but not for the shortest coherence length. The values of R for these three reconstructions are $R = 0.006$, 0.009, and 0.06 respectively. Note, here we used the simulated sample instead of $T^C_{i,j}$ to calculate the R value.

CDI typically requires that[23] $S_s >= 1$ and $S_l > 1$. To achieve these illumination conditions, it is generally necessary to reduce the phase space of the incident beam by including slits to confine the beam and a monochromator to reduce its overall bandwidth. By using knowledge of the lateral and longitudinal coherence in the reconstruction algorithm, we have shown that we can relax the coherence requirements to $S_s > 0.5$ and $S_l > 0.5$, as shown in Fig. 7. By doing so, the required exposure time is significantly decreased. In our experiment, we keep the maximum count of every frame constant at a level that ensures a reasonable dynamic range while retaining linearity of the CCD. The exposure time for the high coherence data is 2 s [the flux is 7.6×10^7 photons/s, Fig. 6(a)], while the exposure time for Fig. 6(d) is 5 ms (the flux is 3.0×10^{10} photons/s), the maximum speed achievable by our shutter. The exposure time is therefore reduced by a factor of 400. In the case of Fig. 6(e), a kapton film with thickness of 51 μm was needed to attenuate the beam to limit exposure (the flux is 3.9×10^{10} photons/s). In this case, the effective improvement of the exposure time is by a factor of about 500. Such a level of improvement opens up significant experimental advantages including real-time imaging, reduced sensitivity to experimental instability and the acquisition of a full CDI tomography data in minutes instead of hours. The spatial resolution of each of the reconstructions was measured by taking a line-out across an edge and was found to be independent of the coherence of the light to within experimental error, and therefore independent of both exposure time and incident flux, for all reconstructions satisfying the requirement $R > 0.04$.

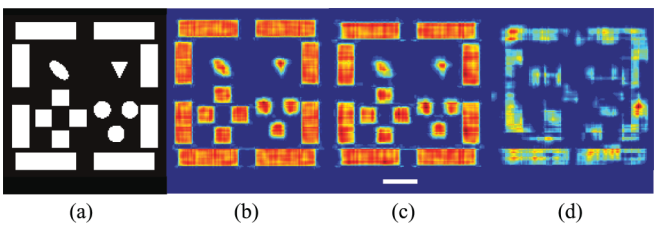

FIG. 8. (Color online) Reconstructed amplitude of the transmission function from simulated data with $S_s = 0.83$. (a) The simulated sample (b) $S_l = 1.67$, (c) $S_l = 0.72$, and (d) $S_l = 0.33$. The scale bar is 2 μm.Color scale is as for Fig. 5 except for (a) where for clarity, a binary image is shown.

VII. CONCLUSION

In this paper, we have experimentally explored the relationship between lateral coherence, longitudinal coherence and the ability to reconstruct an image using the methods of partially coherent diffractive imaging. We have compared our results to the broad criteria proposed by Spence *et al.* and have found that by incorporating the methods of partial coherence into the reconstruction procedure, if the coherence properties are known either a *priori* or through experiment, we may relax these minimal criteria by a factor of 2 in both lateral coherence length and longitudinal coherence length. In practice, we suggest that the improvements are very much more than this as for most objects, other authors have found that the minimal coherence requirements are not sufficient to obtain a reliable imaging approach. We therefore suggest that the results reported in this paper will offer rather more significant gains in experimental implementations of CDI using partially coherent illumination.

ACKNOWLEDGMENT

The authors acknowledge the support of the Australian Research Council Centre of Excellence for Coherent X-ray Science. Use of the Advanced Photon Source was supported by the US Department of Energy, Office of Science, Office of Basic Energy Sciences(contract no. DE-AC02-06CH11357).

*B.Abbey@latrobe.edu.au

[1] J. Miao, P. Charalambous, J. Kirz, and D. Sayre, Nature (London) **400**, 342 (1999).
[2] H. N. Chapman and K. A. Nugent, Nat. Photon. **4**, 833 (2010).
[3] K. A. Nugent, Adv. Phys. **59**, 1 (2010).
[4] I. Robinson and R. Harder, Nat. Mater. **8**, 291 (2009).
[5] Y. Nishino, J. Miao, and T. Ishikawa, Phys. Rev. B **68**, 220101 (2003).
[6] J. Miao, Y. Nishino, Y. Kohmura, B. Johnson, C. Song, S. H. Risbud, and T. Ishikawa, Phys. Rev. Lett. **95**, 085503 (2005).
[7] C. Song, H. Jiang, A. Mancuso, B. Amirbekian, L. Peng, R. Sun, S. S. Shah, Z. H. Zhou, T. Ishikawa, and J. Miao, Phys. Rev. Lett. **101**, 158101 (2008).
[8] G. J. Williams, E. Hanssen, A. G. Peele, M. A. Pfeifer, J. Clark, B. Abbey, G. Cadenazzi, M. D. de Jonge, S. Vogt, L. Tilley, Others, and K. A. Nugent, Cytometry Part A **73**, 949 (2008).
[9] X. Huang, J. Nelson, J. Kirz, E. Lima, S. Marchesini, H. Miao, A. M. Neiman, D. Shapiro, J. Steinbrener, A. Stewart, J. J. Turner, and C. Jacobsen, Phys. Rev. Lett. **103**, 198101 (2009).
[10] J. Nelson, X. Huang, J. Steinbrener, D. Shapiro, J. Kirz, S. Marchesini, A. M. Neiman, J. J. Turner, and C. Jacobsen, Proc. Natl. Acad. Sci. USA **107**, 7235 (2010).
[11] H. Jiang, C. Song, C.-C. Chen, R. Xu, K. S. Raines, B. P. Fahimian, C.-H. Lu, T.-K. Lee, A. Nakashima, J. Urano, T. Ishikawa, F. Tamanoi, and J. Miao, Proc. Natl. Acad. Sci. USA **107**, 11234 (2010).
[12] K. Giewekemeyer, P. Thibault, S. Kalbfleisch, A. Beerlink, C. M. Kewish, M. Dierolf, F. Pfeiffer, and T. Salditt, Proc. Nat. Acad. Sci. USA **107**, 529 (2010).
[13] H. N. Chapman, A. Barty, M. J. Bogan, S. Boutet, M. Frank, S. P. Hau-Riege, S. Marchesini, B. W. Woods, S. Bajt, W. H. Benner, R. A. London, E. Plönjes, M. Kuhlmann, R. Treusch,S. Düsterer *et al.*, Nat. Phys. **2**, 839 (2006).
[14] M. M. Seibert, T. Ekeberg, F. R. N. C. Maia, M. Svenda, J. Andreasson, O. Jönsson, D. Odić, B. Iwan, A. Rocker, D. Westphal, M. Hantke, D. P. DePonte, A. Barty, J. Schulz, L. Gumprecht *et al.*, Nature (London) **470**, 78 (2011).
[15] G. J. Williams, H. M. Quiney, A. G. Peele, and K. A. Nugent, Phys. Rev. B **75**, 104102 (2007).
[16] I. Vartanyants, A. Singer, A. Mancuso, O. Yefanov, A. Sakdinawat, Y. Liu, E. Bang, G. Williams, G. Cadenazzi, B. Abbey, H. Sinn, D. Attwood, K. Nugent, E. Weckert, T. Wang, Zhu *et al.*, Phys. Rev. Lett. **107**, 144801 (2011).
[17] L. W. Whitehead, G. J. Williams, H. M. Quiney, D. J. Vine, R. A. Dilanian, S. Flewett, K. A. Nugent, A. G. Peele, E. Balaur, and I. McNulty, Phys. Rev. Lett. **103**, 243902 (2009).
[18] B. Chen, R. A. Dilanian, S. Teichmann, B. Abbey, A. G. Peele, G. J. Williams, P. Hannaford, L. Van Dao, H. M. Quiney, and K. A. Nugent, Phys. Rev. A **79**, 023809 (2009).
[19] B. Abbey, L. W. Whitehead, H. M. Quiney, D. J. Vine, G. A. Cadenazzi, C. A. Henderson, K. A. Nugent, E. Balaur, C. T. Putkunz, A. G. Peele, and Others, Nat. Photon. **5**, 420 (2011).
[20] E. Wolf, J. Opt. Soc. Am. **72**, 343 (1982).
[21] C. Q. Tran, G. J. Williams, A. Roberts, S. Flewett, A. G. Peele, D. Paterson, M. D. de Jonge, and K. A. Nugent, Phys. Rev. Lett. **98**, 224801 (2007).
[22] S. Flewett, H. M. Quiney, C. Q. Tran, and K. A. Nugent, Opt. Lett. **34**, 2198 (2009).
[23] J. C. H. Spence, U. Weierstall, and M. Howells, Ultramicroscopy **101**, 149 (2004).
[24] L. W. Whitehead, G. J. Williams, H. M. Quiney, K. A. Nugent, A. G. Peele, D. Paterson, M. D. de Jonge, and I. McNulty, Phys. Rev. B **77**, 104112 (2008).
[25] A. Starikov and E. Wolf, J. Opt. Soc. Am. **72**, 923 (1982).
[26] R. A. Bartels, A. Paul, M. M. Murnane, H. C. Kapteyn, and S. Backus, Opt. Lett. **27**, 707 (2002).
[27] R. A. Dilanian, B. Chen, S. Teichmann, L. Van Dao, H. M. Quiney, K. A. Nugent, and L. Dao, Opt. Lett. **33**, 2341 (2008).
[28] J. R. Fienup, Appl. Opt. **21**, 2758 (1982).
[29] G. Oszlányi and A. Süto, Acta Crystallogr. Sect. A **64**, 123 (2008).
[30] S. Marchesini, H. He, H. N. Chapman, S. P. Hau-Riege, A. Noy, M. R. Howells, U. Weierstall, and J. C. H. Spence, Phys. Rev. B **68**, 140101(R) (2003).
[31] I. McNulty, A. Khounsary, Y. P. Feng, Y. Qian, J. Barraza, C. Benson, and D. Shu, Rev. Sci. Instrum. **67**, 3372 (1996).
[32] D. Vine, G. Williams, J. Clark, C. Putkunz, M. Pfeifer, D. Legnini, C. Roehrig, E. Wrobel, E. Huwald, G. van Riessen, B. Abbey, T. Beetz, J. Irwin, M. Freser, H. B., I. McNulty, K. Nugent, and A. Peel, Rev. Sci. Instrum. **83**, 033703 (2012).
[33] D. Paterson, B. E. Allman, P. J. McMahon, J. Lin, N. Moldovan, K. A. Nugent, I. McNulty, C. T. Chantler, C. C. Retsch, T. H. K. Irving, and D. C. Mancini, Opt. Commun. **195**, 79 (2001).